

## The Dir meta-volcanic sequence: Calcalkaline magmatism in the Kohistan Arc terrane, northern Pakistan

M. TAHIR SHAH<sup>1</sup>, JOHN W. SHERVAIS<sup>2</sup> & MOHAMMED IKRAMUDDIN<sup>3</sup>

<sup>1</sup>NCE in Geology University of Peshawar

<sup>2</sup>Department of Geological Sciences, University of South Carolina, USA

<sup>3</sup>Department of Geology, Eastern Washington University, USA

**ABSTRACT:** A variably deformed and metamorphosed NE-SW trending belt of Dir metavolcanic sequence is exposed within the north-western portion of the Kohistan arc terrane. The sequence is mainly composed of massive and sheared volcanics and pyroclastic breccia. The petrochemical indices suggest that they are dominantly basaltic-andesite and andesite with subordinate basalt, dacite and rhyolite in composition.

Whole rock major element compositions define a calc-alkaline trend: CaO, FeO, MgO, TiO<sub>2</sub>, Al<sub>2</sub>O<sub>3</sub>, V, Cr, Ni, and Sc all decrease with increasing silica, whereas alkalis, Rb, Ba, and Y increase. Mafic to intermediate volcanic rocks show calc-alkaline affinities on petrochemical diagrams. Chondrite-normalized REE patterns are LREE-enriched. Dacites and rhyolites have the lowest La/Lu ratios and highest Eu/Eu\* ratios, reflecting the dominant role of plagioclase fractionation in their formation. MORB-normalized spider diagrams show progressive enrichment of the low-field strength incompatible elements (Ce, La, Ba, Rb, K) and a distinct negative Nb anomaly; patterns typical of subduction related magmas.

It is suggested that the high-Mg basalt of the Dir area is primitive in nature and could be the representative of the primary magnesian liquid formed by the partial melting of mantle wedge at the base of the Kohistan arc terrane. This liquid may have fractionated the other members of the sequence especially low magnesia basalt and basaltic-andesite.

### INTRODUCTION

The Kohistan arc terrane in the northern part of Pakistan represents an island arc sequence, developed prior to the suturing of the Indo-Pakistan and Asiatic plates. The Kohistan island arc is bounded by two major faults: the Northern Suture or Main Karakoram Thrust (MKT) in the north and Main Mantle Thrust (MMT) in the south (Fig. 1). These faults separate arc rocks of the Kohistan terrane from continental rocks of the Asiatic plate to the

north and the Indo-Pakistan plate to the south. Both the MMT and MKT are characterized by discontinuous outcrops of ophiolite in serpentinite or shale-matrix melanges (Tahirkheli et al., 1979; Bard, 1983; Coward et al., 1986; Pudsey, 1986; Hanson, 1989).

The Dir metavolcanic sequence is a part of the Dir-Utror volcanic series within the Kohistan island arc. The Dir-Utror volcanic series, found only in the west-central part of the Kohistan terrane, forms a ENE-WSW

trending belt from Utror through Dir to the border of Afghanistan (Fig. 1). These volcanics and associated metasediments have been interpreted as a part of the Kohistan island arc (Tahirikheli et al, 1979; Majid & Paracha, 1980; Majid et al, 1981). Tahirikheli (1979, 1982) described the Dir-Utror volcanics and associated metasediments as member of the Dir group and suggested a middle Jurassic to Cretaceous age for the metasediments. Whereas Kakar et al. (1971), Khan (1979) and Treloar et al. (1988) assigned a late Palaeocene to early Eocene age to the Dir group on the basis of palaeontological and radiometric studies. Recent studies of Hamidullah and Onstot (1992) based on  $^{40}\text{Ar}/^{39}\text{Ar}$  data of primary hornblende from an andesite support the former date.

The Dir-Utror volcanics have been variously described as Utror volcanics at Utror (upper Swat) (Majid & Paracha, 1980) and part of the Kalam-Dir igneous complex (Hamidullah et al., 1990). These studies describe these volcanics to be subduction related calc-alkaline type. Fletcher (1985) regarded these to be Within Plate Basalt type of lavas. However, Sullivan (1993) has documented their arc-related affinities with magma generation along continental margin.

The present study provide further data to describes the detailed geochemical characteristics of the Dir metavolcanic sequence in order to understand the origin and type of tectonic environment for the development of this sequence within the Kohistan arc terrane.

## GEOLOGY OF THE AREA

The area of study is located along the Dir-Chitral road near Dir town in northern Pakistan. Its geology is characterized by a sequence of metavolcanic, metasedimentary and plutonic rocks. A variably metamorphosed volcanic sequence containing copper mineralization, is

exposed in the area (Shah et al., 1990; Shah & Shervais, 1991). This sequence is part of the northeast-southwest trending belt of volcanic rocks exposed in the north western portion of the Kohistan island arc.

The Dir metavolcanic sequence generally has upper thrust contact with the quartz diorites of the Lowari pluton. However, in the studied area the sequence has an upper thrust contact with the Panakot meta-arkosic sandstone which inturn has an upper thrust contact with the quartz diorites of the Lowari pluton (Fig. 1). The sequence has a lower thrust contact with the epiclastic siltstone (Fig. 1). The metavolcanic sequence in the area is mainly composed of basaltic-andesite and andesite with subordinate basalt, dacite, rhyolite and pyroclastic breccia (Shah et al., 1990; Shah & Shervais, 1991). These rocks have been intruded by small plugs and dikes of diorite to granodiorite composition. The metavolcanics in general have been subjected to greenschist-facies metamorphism, however, epidote-amphibolite facies conditions attained locally, have also been reported (Shah & Hamidullah, 1993) in places. Basaltic-andesites and andesites are the most voluminous rocks exposed in the area. These fine-grained, greenish-gray to green rocks are foliated. These commonly have relict porphyritic textures but are schistose adjacent to faults. Plagioclase is the dominant phenocryst however rare phenocrysts of primary hornblende have also been reported in one sample from Dir area (Hamidullah & Shah, 1993). Plagioclase, epidote, chlorite, actinolite, rare hornblende, and opaques comprise the ground mass. Metarhyolite and metadacite occur as small outcrops in the southwestern part of the area. These fine-grained, light-gray foliated rocks consist of quartz and feldspar (both as phenocryst and in the groundmass) with mica (muscovite and biotite), sericite, epidote, chlorite, and

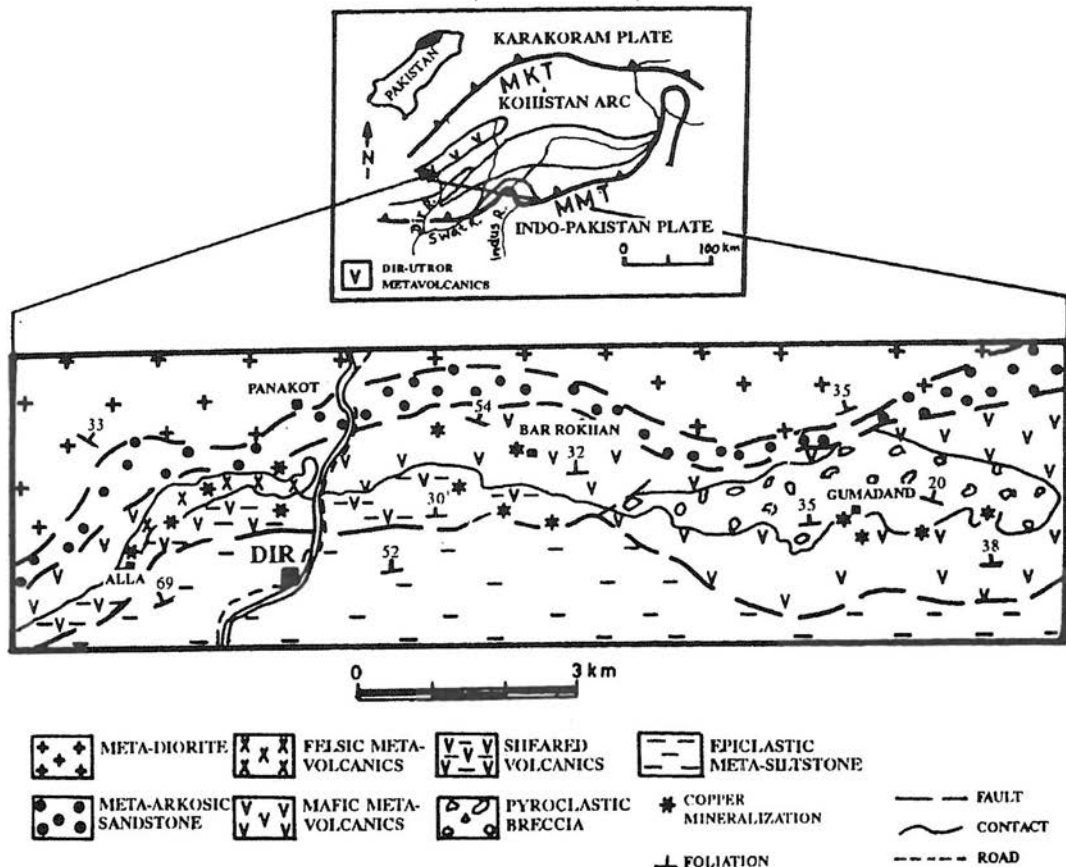


Fig. 1. Geological map of the area around Dir, northern Pakistan.

opaque as minor phases in the fine-grained groundmass. Maroon-colored pyroclastic breccia is exposed in the northeastern part of the area. Normally these rocks are composed of poly-mict, matrix-supported breccia. But towards the central part of the area clast-supported breccia (possibly representing a near vent facies) has also been noticed.

Hydrothermal alteration occurs in localized zones of intense faulting and shearing which facilitated movement of the copper-bearing hydrothermal solutions. These hydrothermal solutions resulted in the deposition of mineralized quartz veins, alteration of adjacent metavolcanic host rock, and precipitation of

copper-bearing phases in the host rock. The oxygen isotope studies suggest the involvement of oxygen enriched heavy fluid in the alteration and copper mineralization within the sequence at depth (Shah, 1991).

#### WHOLE ROCK GEOCHEMISTRY

Sixty of the least altered samples, representing every major rock unit of the Dir metavolcanic sequence, have been analyzed for major and trace elements. The results of the selected samples from each unit are listed in Tables 1 and 2. One representative sample from each unit has been analyzed for rare earth elements (Table 3). Major and trace element concentra-

TABLE 1. REPRESENTATIVE CHEMICAL ANALYSES OF THE SELECTED ROCKS FROM THE DIR METAVOLCANIC SEQUENCE, NORTHERN PAKISTAN.

S.NO	BASALTS AND BASALTIC ANDESITES													ANDESITES				
	DR 117	DR 467	DR 400	DR 493	DR 321	DR 508	DR 389	DR 383	DR 131	DR 360	DR 263	DR 512	DR 197	DR 10				
SiO <sub>2</sub>	49.45	47.39	50.83	51.29	50.61	52.94	50.58	50.46	48.52	48.17	58.93	58.48	55.81	57.81				
TiO <sub>2</sub>	1.03	1.04	0.92	0.82	0.65	0.69	0.66	0.68	0.99	1.35	0.67	0.74	0.77	0.84				
Al <sub>2</sub> O <sub>3</sub>	15.1	15.14	18.31	15.63	19.07	14.87	19.43	17.79	14.96	20.14	16.20	17.50	14.76	17.47				
Fe <sub>2</sub> O <sub>3</sub>	8.88	10.86	9.36	8.26	7.79	9.07	7.70	10.00	9.41	10.00	5.71	6.63	6.70	5.47				
MnO	0.19	0.21	0.15	0.10	0.16	0.17	0.15	0.21	0.22	0.16	0.12	0.09	0.27	0.14				
MgO	9.46	13.22	6.02	7.31	5.69	5.11	3.63	8.06	7.12	11.42	2.44	3.70	3.44	1.22				
CaO	6.86	5.90	5.49	6.69	5.65	7.92	6.75	4.46	7.54	3.34	6.37	4.39	6.18	4.12				
Na <sub>2</sub> O	4.52	2.27	3.28	3.56	4.39	2.75	2.59	4.70	3.02	3.77	3.63	1.23	4.11	4.42				
K <sub>2</sub> O	0.25	0.05	1.56	1.49	0.63	1.37	2.95	0.90	0.95	1.23	2.06	3.62	3.55	4				
P <sub>2</sub> O <sub>5</sub>	0.22	0.38	0.18	0.25	0.29	0.24	0.32	0.22	0.31	0.26	0.22	0.16	0.26	0.36				
LOI	5.21	4.88	3.23	4.86	3.86	3.78	6.06	4.28	5.43	2.12	2.59	2.88	2.89	2.86				
Total	101.2	101.34	99.33	100.26	98.79	98.91	100.82	101.76	98.47	101.96	98.94	99.42	98.74	98.71				
Trace elements in ppm																		
Nb	4	11	5	0	8	12	11	0	4	14	12	9	11	10				
Zr	140	158	96	115	128	94	137	107	143	134	164	159	150	201				
Y	24	28	25	19	29	20	30	20	25	28	21	30	25	38				
Sr	322	704	288	528	884	361	403	331	356	250	479	182	251	392				
Rb	8	0	40	56	16	36	58	28	25	34	52	153	85	100				
Ni	47	150	40	16	8	20	17	30	37	55	24	50	33	0				
Cr	106	362	57	35	14	30	23	48	57	155	33	58	74	8				
V	227	315	272	274	153	211	180	263	294	300	162	137	155	65				
Sc	23	34	21	26	15	22	14	26	26	23	18	15	16	14				
Ba	24	9	472	101	94	341	329	164	169	101	290	229	468	477				
Zn	132	114	87	88	110	103	114	118	139	145	108	113	192	161				
Cu	13	110	0	13	25	30	58	54	66	12	18	10	88	14				

(Table 1 continued)

S.NO	DACITES			RHYOLITES			PYROCLASTIC BRECCIA		
	DR 286	DR 192	DR 34A	DR 78	DR 230	DR 218A	DR 398	DR 328	DR 431
SiO <sub>2</sub>	67.80	66.71	64.36	70.52	72.20	71.24	54.04	48.78	53.79
TiO <sub>2</sub>	0.52	0.79	0.61	0.22	0.40	0.34	0.85	0.89	0.86
Al <sub>2</sub> O <sub>3</sub>	15.90	15.23	14.23	14.93	12.94	13.45	19.62	19.54	18.90
Fe <sub>2</sub> O <sub>3</sub>	2.35	2.57	5.06	2.53	2.22	3.45	6.86	9.55	8.96
MnO	0.05	0.15	0.21	0.06	0.08	0.13	0.13	0.17	0.17
MgO	0.43	0.33	1.23	1.57	0.37	0.98	3.75	6.89	8.10
CaO	0.98	0.59	1.06	0.32	2.97	2.56	4.38	6.97	2.94
Na <sub>2</sub> O	6.19	3.86	1.25	7.68	4.58	4.67	5.54	4.14	3.60
K <sub>2</sub> O	3.08	6.52	8.18	1.34	2.29	1.78	1.94	1.79	1.01
P <sub>2</sub> O <sub>5</sub>	0.11	0.22	0.15	0.18	0.11	0.16	0.22	0.25	0.16
LOI	2.04	1.75	2.65	1.65	1.34	1.78	2.13	2.12	3.45
Total	99.45	98.72	98.99	101.00	99.50	100.54	99.46	101.09	101.94
Trace elements in ppm									
Nb	14	12	12	7	7	2	3	7	0
Zr	260	204	193	146	173	214	153	99	90
Y	43	39	36	23	35	21	29	26	21
Sr	119	56	71	47	110	126	335	297	486
Rb	71	78	56	7	53	73	39	63	32
Ni	3	1	4	9	4	13	5	29	63
Cr	6	5	5	11	6	18	17	25	57
V	30	20	78	11	35	98	168	216	247
Sc	11	9	14	5	11	8	16	21	24
Ba	310	599	467	5	97	194	296	150	190
Zn	99	80	89	94	62	96	107	130	121
Cu	12	22	42	17	19	14	20	13	24

TABLE 2. REPRESENTATIVE GEOCHEMICAL DATA (ON ANHYDROUS BASIS) OF THE ROCKS OF THE DIR META VOLCANIC SEQUENCE, NORTHERN PAKISTAN.

HIGH MAGNESIA BASALT				LOW MAGNESIA BASALT				BASALTIC-ANDESITES				
S.Nos.	DR117A	DR 360	DR 467	S.Nos.	DR 131	DR 400	DR 383	S.Nos.	DR 493	DR 321	DR 508	DR 389
SiO <sub>2</sub>	51.53	48.25	49.13	SiO <sub>2</sub>	52.15	52.89	51.76	SiO <sub>2</sub>	53.76	53.31	55.65	53.38
TiO <sub>2</sub>	1.07	1.35	1.08	TiO <sub>2</sub>	1.06	0.96	0.70	TiO <sub>2</sub>	0.86	0.68	0.73	0.70
Al <sub>2</sub> O <sub>3</sub>	15.74	20.17	15.70	Al <sub>2</sub> O <sub>3</sub>	16.08	19.05	18.25	Al <sub>2</sub> O <sub>3</sub>	16.38	20.09	15.63	20.50
Fe <sub>2</sub> O <sub>3</sub>	9.25	10.02	11.26	Fe <sub>2</sub> O <sub>3</sub>	10.11	9.74	10.26	Fe <sub>2</sub> O <sub>3</sub>	8.66	8.21	9.53	8.13
MnO	0.20	0.16	0.22	MnO	0.24	0.16	0.22	MnO	0.10	0.17	0.18	0.16
MgO	9.86	11.44	13.71	MgO	7.65	6.26	8.27	MgO	7.66	5.99	5.37	3.83
CaO	7.15	3.35	6.12	CaO	8.10	5.71	4.58	CaO	7.01	5.95	8.33	7.12
Na <sub>2</sub> O	4.71	3.78	2.35	Na <sub>2</sub> O	3.25	3.41	4.82	Na <sub>2</sub> O	3.73	4.62	2.89	2.73
K <sub>2</sub> O	0.26	1.23	0.05	K <sub>2</sub> O	1.02	1.62	0.92	K <sub>2</sub> O	1.56	0.66	1.44	3.11
P <sub>2</sub> O <sub>5</sub>	0.23	0.26	0.39	P <sub>2</sub> O <sub>5</sub>	0.33	0.19	0.23	P <sub>2</sub> O <sub>5</sub>	0.26	0.31	0.25	0.34
C.P.P.W norms				C.I.P.W norms				C.I.P.W norms				
Or	1.55	7.35	0.31	Q	—	0.51	—	Q	—	—	5.99	1.06
Ab	40.14	32.2	20.09	Or	6.1	9.69	5.51	Or	9.31	3.96	8.59	18.55
An	21.17	15.04	28.08	Ab	27.69	29.1	41.13	Ab	31.79	39.38	24.64	23.27
C	—	7.22	1.59	An	26.49	27.38	21.44	An	23.49	27.76	25.6	33.41
Di	10.56	—	—	C	—	1.73	1.54	C	—	1.66	—	0.47
wo	5.47	—	—	Di	9.7	—	—	Di	8	—	11.87	—
en	3.54	—	—	wo	4.97	—	—	wo	4.12	—	6.02	—
fs	1.55	—	—	en	2.91	—	—	en	2.53	—	3.13	—
Hy	0.26	14.56	35.91	fs	1.82	—	—	fs	1.35	—	2.72	—
en	0.18	10.45	25.8	Hy	21.42	27.42	7.29	Hy	17.7	19.57	19.48	19.56
fs	0.08	4.11	10.12	en	13.17	15.8	4.51	en	11.56	11.75	10.42	9.65
Ol	21.93	18.47	8.85	fs	8.25	11.63	2.78	Ol	5.79	4.07	—	—
fo	14.79	12.88	6.18	Ol	3.83	—	19.24	fs	6.14	7.82	9.06	9.91
fa	7.14	5.59	2.67	fo	2.26	—	11.45	fo	3.65	2.35	—	—
Mt	1.83	1.98	2.23	fa	1.56	—	7.79	fa	2.14	1.72	—	—
Il	2.06	2.59	2.07	Mt	2	1.92	2.03	Mt	1.71	1.62	1.88	1.6
Ap	0.5	0.57	0.87	Il	2.04	1.83	1.34	Il	1.65	1.31	1.39	1.33
				Ap	0.73	0.41	0.5	Ap	0.58	0.67	0.56	0.74
Mg#	67.87	69.35	70.69	Mg#	59.99	56.03	61.49	Mg#	63.68	59.14	52.75	48.29

(Table 2 continued)

ANDESITES					DACITES				RHYOLITES				PYROCLASTIC BRECCIA			
S.Nos.	DR	DR	DR	DR	S.Nos.	DR	DR	DR	SNos.	DR	DR	DR	S.Nos.	DR	DR	DR
	263	309	197	10		47	192	34A		78	230	218A		398	328	431
SiO <sub>2</sub>	61.16	59.19	58.23	60.31	SiO <sub>2</sub>	68.15	68.79	66.81	SiO <sub>2</sub>	70.98	73.55	72.13	SiO <sub>2</sub>	55.52	49.29	54.61
TiO <sub>2</sub>	0.70	0.68	0.80	0.88	TiO <sub>2</sub>	0.44	0.81	0.63	TiO <sub>2</sub>	0.22	0.41	0.34	TiO <sub>2</sub>	0.87	0.90	0.87
Al <sub>2</sub> O <sub>3</sub>	16.81	18.25	15.40	18.23	Al <sub>2</sub> O <sub>3</sub>	15.61	15.71	14.77	Al <sub>2</sub> O <sub>3</sub>	15.03	13.18	13.62	Al <sub>2</sub> O <sub>3</sub>	20.16	19.74	19.19
Fe <sub>2</sub> O <sub>3</sub>	5.93	6.66	6.99	5.71	Fe <sub>2</sub> O <sub>3</sub>	5.75	2.65	5.25	Fe <sub>2</sub> O <sub>3</sub>	2.55	2.26	3.49	Fe <sub>2</sub> O <sub>3</sub>	7.05	9.65	9.10
MnO	0.12	0.09	0.28	0.15	MnO	0.15	0.15	0.22	MnO	0.06	0.08	0.13	MnO	0.13	0.17	0.17
MgO	2.53	3.23	3.59	1.27	MgO	2.61	0.34	1.28	MgO	1.58	0.38	0.99	MgO	3.85	6.96	8.22
CaO	6.61	6.00	6.45	4.30	CaO	0.25	0.61	1.10	CaO	0.32	3.03	2.59	CaO	4.50	7.04	2.99
Na <sub>2</sub> O	3.77	1.34	4.29	4.61	Na <sub>2</sub> O	6.63	3.98	1.30	Na <sub>2</sub> O	7.73	4.46	4.73	Na <sub>2</sub> O	5.69	4.18	3.66
K <sub>2</sub> O	2.14	4.38	3.70	4.17	K <sub>2</sub> O	0.29	6.72	8.49	K <sub>2</sub> O	1.35	2.33	1.80	K <sub>2</sub> O	1.99	1.81	1.03
P <sub>2</sub> O <sub>5</sub>	0.23	0.18	0.27	0.38	P <sub>2</sub> O <sub>5</sub>	0.13	0.23	0.16	P <sub>2</sub> O <sub>5</sub>	0.18	0.11	0.16	P <sub>2</sub> O <sub>5</sub>	0.23	0.25	0.16
C.I.P.W norms					C.I.P.W norms				C.I.P.W norms				C.I.P.W norms			
Q	12.06	13.94	0.88	5.12	Q	21.36	17.7	20.16	Q	17.01	31.08	29.61	Q	—	—	6.31
Or	12.72	26.08	22.05	24.82	Or	1.73	39.87	50.46	Or	8	13.83	10.07	Or	11.87	10.79	6.11
Ab	32.01	11.04	36.47	39.19	Ab	56.29	33.73	11.02	Ab	65.49	39.52	40.09	Ab	48.42	27.38	31.14
An	22.73	28.82	11.87	16.75	An	0.36	1.55	4.47	An	0.42	8.13	10.62	An	21	29.96	13.87
C	—	0.78	—	—	C	4.28	1.3	1.8	C	0.7	—	—	Ne	—	4.49	—
Di	7.27	—	15.31	1.9	Hy	13.73	3.29	9.51	Di	—	5.29	1.04	C	0.98	—	7.07
wo	3.66	—	7.75	0.94	en	6.57	0.85	3.21	wo	—	2.58	0.51	Di	—	2.97	—
en	1.73	—	3.91	0.32	fs	7.16	2.44	6.3	en	—	0.75	0.19	wo	—	1.52	—
fs	1.88	—	3.66	0.64	Mt	1.13	0.52	1.03	fs	—	1.95	0.33	en	—	0.87	—
Hy	9.67	15.98	9.91	8.6	Il	0.83	1.55	1.21	Hy	7.07	0.7	6.25	fs	—	0.58	—
en	4.64	8.12	5.12	2.88	Ap	0.3	0.5	0.34	en	3.96	0.19	2.3	Hy	4.17	—	31.67
fs	5.04	7.86	4.79	5.73	Mg#	47.36	20.28	32.51	fs	3.1	0.51	3.96	en	2.27	—	20.73
Mt	1.17	1.31	1.38	1.12					Mt	0.5	0.44	0.69	fs	1.9	—	10.94
Il	1.33	1.3	1.54	1.67					Il	0.42	0.78	0.66	OI	10.01	20.22	—
Ap	0.5	0.38	0.6	0.82					Ap	0.4	0.25	0.35	fo	5.2	11.68	—
													fa	4.81	8.54	—
Mg#	45.85	48.98	50.43	30.65					Mg#	55.51	24.82	36.01	Mt	1.39	1.9	1.79
													Il	1.67	1.72	1.67
													Ap	0.5	0.56	0.36
													Mg#	51.99	58.84	64.17

TABLE 3. REE ANALYSES AND INTERELEMENT RATIOS FOR SELECTED SAMPLES FROM EACH UNIT OF THE DIR METAVOLCANIC SEQUENCE.

	Basalt	Pyroclastic breccia	Basaltic andesite	Andesite	Dacite	Rhyolite
	DR311	DR398	DR350	DR263	DR192	DR29
La	9.50	11.20	11.60	12.00	17.40	20.25
Ce	21.40	25.70	25.85	27.10	43.10	47.50
Nd	8.60	11.85	11.30	12.35	20.20	21.40
Sm	1.75	2.70	2.75	3.15	6.15	6.35
Eu	0.51	0.63	0.70	0.68	0.93	0.98
Gd	2.35	2.55	2.45	2.85	5.15	5.40
Dy	2.10	3.55	3.06	3.37	6.32	5.86
Yb	1.10	1.88	1.72	1.93	4.34	3.50
Lu	0.16	0.22	0.24	0.26	0.67	0.51
(La/Lu)N	6.12	5.77	5.09	4.85	2.70	4.13
Eu/Eu*	0.86	0.74	0.82	0.69	0.51	0.51

Element ratios are chondrite-normalized after Nakamura (1974).

tions were determined on pressed powdered pellets using a fully automated Phillips PW-1400 X-ray fluorescence (XRF) at the University of South Carolina. Calibration lines were constructed using up to 15 recommended U.S.G.S standards. Samples for REE analyses were prepared using an ion-exchange technique following the method of Crock and Lichte (1982) and analyzed on ICP (inductively coupled plasma) spectrometer at the Eastern Washington University. Loss of ignition (LOI) was performed in duplicate by heating about 2g sample at 950°C for more than four hours.

The high loss of ignition (up to 6%) suggests that water content has been increased by either low grade regional metamorphism or sea water interaction. As a result the major oxides data of Table 1 have been recalculated to 100%

on volatile free basis (Table 2) to eliminate any complication due to higher loss of ignition in these rocks. These data (Table 2) has been used for further interpretation and comparison. The CIPW norms shown in Table 2 are based on  $Fe_2O_3/FeO$  ratio = 0.15.

#### Major elements

The rocks of the sequence are classified on the basis of  $SiO_2$  contents (Gill, 1981) as basalts (<53 wt.%  $SiO_2$ ), basaltic-andesites (53-57 wt %  $SiO_2$ ), andesites (57-63 wt.%  $SiO_2$ ), dacites (63-70 wt.%  $SiO_2$ ) and rhyolites (>70 wt.%  $SiO_2$ ). The pyroclastic rocks are mostly basalt or basaltic-andesites (Table 2) and have been treated separately in all the diagrams to show their relationship with lavas of similar composition from Dir area.

The basalts have been divided into two main classes on the basis of MgO contents: (a) high-magnesia basalt with MgO contents >9 wt.% and (b) low-magnesia basalts or transitional basalt with MgO contents <9 wt.% (see Myers, 1988). The high-magnesia basalts show a wider variation in the MgO contents between 9.86 to 13.71 wt.% with an average of 11.89 wt.%. On the other hand the low-magnesia basalts have narrower range (6.39 to 8.27 wt.%) with an average of 6.99 wt.%. The  $\text{Fe}_2\text{O}_3$ ,  $\text{Na}_2\text{O}$  and  $\text{P}_2\text{O}_5$  contents are similar in both the high-magnesia basalt and the low-magnesia basalts but the other oxides (i.e.  $\text{SiO}_2$ ,  $\text{Al}_2\text{O}_3$ ,  $\text{CaO}$ ,  $\text{K}_2\text{O}$ ) are lower in the former type. Among the trace elements, Rb and Ba are enriched and Sr, Sc, Cr and Ni are depleted in latter type as compared to the former.

The major element data for the Dir metavolcanic sequence are plotted on conventional Harker variation diagrams (Fig. 2). The data points approximate a liquid line of descent from basalt to rhyolite, although most oxides show some scatter. MgO,  $\text{Fe}_2\text{O}_3$ ,  $\text{TiO}_2$ ,  $\text{CaO}$  and  $\text{P}_2\text{O}_5$  all show negative correlation with  $\text{SiO}_2$ . Important is the lack of iron enrichment which is the characteristic feature of calc-alkaline rocks.  $\text{Al}_2\text{O}_3$  shows a vague negative correlation against  $\text{SiO}_2$  with some scatter in the basalt to basaltic-andesites.  $\text{Na}_2\text{O}$  and  $\text{K}_2\text{O}$  show considerable scatter against  $\text{SiO}_2$  (Figs. 2f, g), but the total alkalis vs  $\text{SiO}_2$  plot exhibit a relatively smooth trend indicating enrichment from basalt to rhyolite (Fig. 2h). This is probably related to complementary replacement of these two oxides for each other in various phases.  $\text{CaO}$  shows a considerable scatter against  $\text{SiO}_2$  (Fig. 2e). The greater scatter of  $\text{Na}_2\text{O}$ ,  $\text{K}_2\text{O}$  and  $\text{CaO}$  can be attributed to the gain or loss of these oxides during low grade regional metamorphism or later alteration.

On the AFM plot (Fig. 3) most samples fall in the calc-alkaline field, and the whole

series exhibits a typical none iron enrichment trend. It is clear from Table 2 that all high-magnesia basalts and the majority of low-magnesia basalts and pyroclastic breccias are silica-undersaturated (olivine normative). Most of the basaltic-andesites (except two analyses) and andesites are silica-saturated (quartz normative). Corundum is present in the norms of some of the basalts, pyroclastic breccias, basaltic-andesites, andesites, and rhyolites, though it is ubiquitous in the norms of dacites (Table 2).

### Trace elements

The trace element data are plotted against silica (Fig. 4) and other major element oxides for which they substitute during magmatic differentiation (Fig. 5). The trends shown by most of the trace elements are consistent with the operation of fractional crystallization. There are strong negative correlations shown by Cr, Ni, V and Sc against  $\text{SiO}_2$ , indicating concentration in crystallizing phases (Fig. 4). On the other hand Rb and Ba vs  $\text{SiO}_2$  plots show scatter with vague positive correlations indicating enrichment in residual liquid. Y shows a more or less constant trend from basalt to dacite with a slight increase from dacite to rhyolite. Despite a considerable scatter seen on Sr vs  $\text{SiO}_2$  plot the over all trend is negative and shows depletion from basalt to rhyolite. This can be attributed to the variable degree of plagioclase fractionation as well as alteration phenomenon.

Cr and Ni vs MgO, and V and Sc vs  $\text{Fe}_2\text{O}_3$  plots show positive correlations reflecting the partitioning of these elements in ferromagnesian minerals (Fig. 5a, b, c & d). On the other hand Rb shows, in general, a steady increase in concentration with K, however, both do not follow the general evolutionary trend from basalt through dacite to rhyolite (Fig. 5e). This feature can be attributed to the crystallization of K-rich and-poor phases at

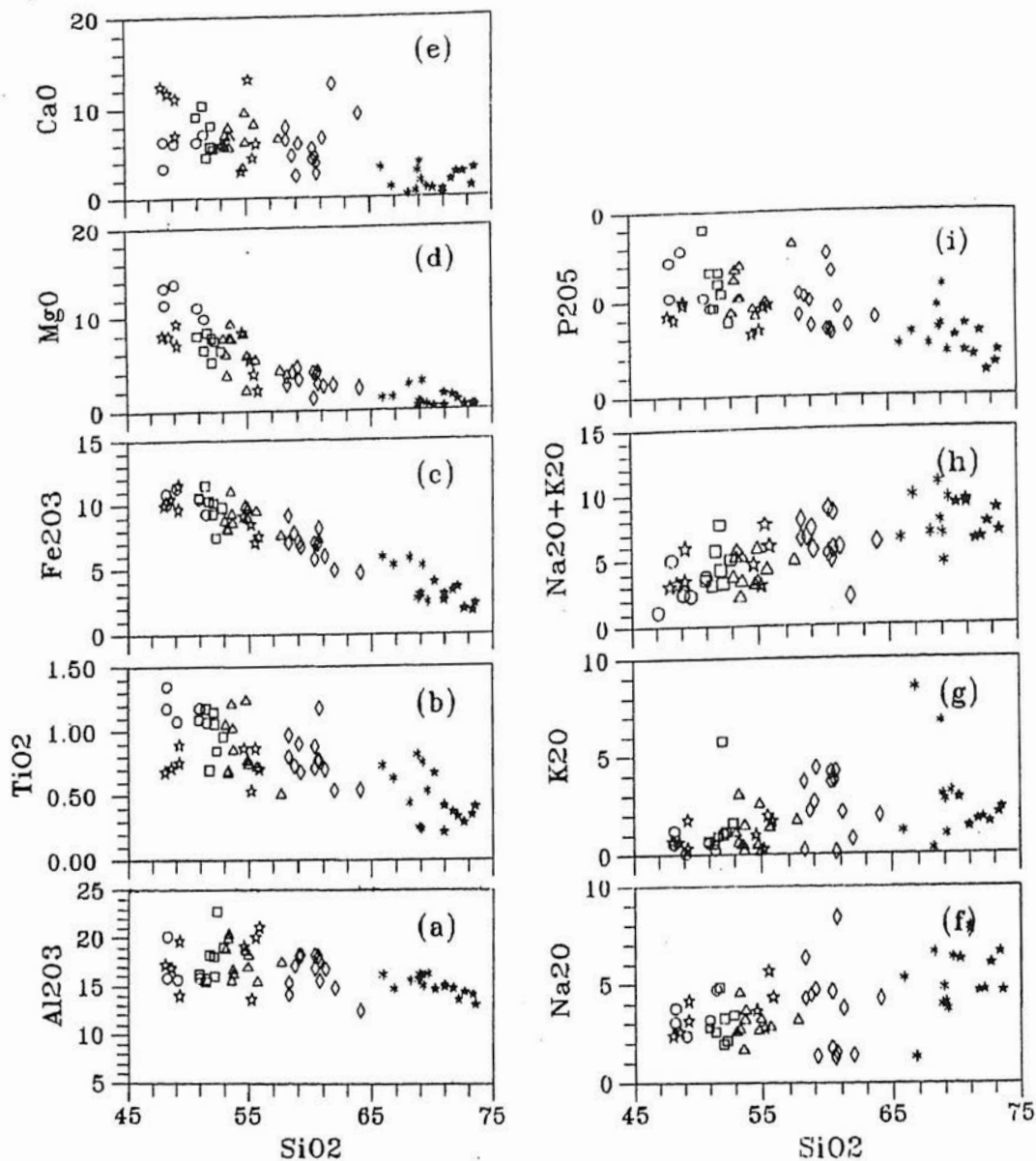


Fig. 2. Variation diagrams of major elements vs silica for the rocks of the Dir metavolcanic sequence. Symbols: o = high-Mg basalt, □ = low-Mg basalt, ☆ = pyroclastic breccia, Δ = basaltic-andesite, ◇ = andesite, \* = dacite, ★ = rhyolite.

different stages of fractionation as well as to the mobility of these elements during low grade metamorphism.

#### Rare Earth Elements

Selected samples from each rock type (except high-magnesia basalt) of the Dir metavolcanic

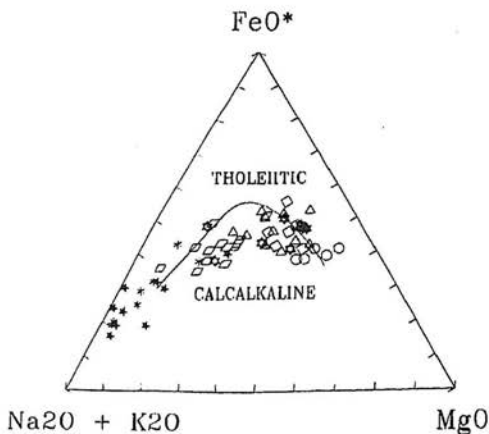


Fig. 3. AFM diagram for the rocks of the Dir metavolcanic sequence. Fields are after Irvine and Baragar, (1971). (Symbols as for Fig. 2).

sequence have been analyzed for the nine rare earth element (REE); the data are listed in Table 3. Chondrite normalized REE patterns for each member, calculated using Nakamura's (1974) chondrite values, for each member are shown in Fig. 6. All the members of the sequence are enriched in light rare earth elements (LREE) compared to the heavy rare earth elements (HREE). Except for Eu anomalies, all the members of the Dir metavolcanic sequence exhibit trends typical of calc-alkaline rocks (Gill, 1981). The sequence shows variable enrichment of LREE to HREE, expressed as the chondrite-normalized ratio  $(La/Lu)_N$ , which ranges from 6.12 (in basalt) to 4.13 (in rhyolites). The pyroclastic rocks have chondrite normalized pattern similar to those of basalt and basaltic-andesites (Fig. 6). The total REE abundances increase systematically from basalt to rhyolites and can be explained in terms of fractional crystallization. However, a decrease in  $La/Lu$  ratio may correspond to the large amount of plagioclase fractionation in acidic rocks.

The measured Eu anomalies, defined as  $Eu_N/Eu^*$  where  $Eu_N$  is the chondrite normalized Eu and  $Eu^*$  is the straight-line interpolation

between plotted points for Sm and Gd i.e.  $[(Sm_N + Gd_N)/2]$ , are also consistent with a magmatic fractionation model. The negative Eu anomaly systematically becomes larger from basalt to rhyolite. If this Eu anomaly is not the result of primary geochemical variation, then plagioclase fractionation at low pressure has played a major role in fractionation of these rocks. As calcic-plagioclase in the studied rocks has mostly been replaced by albite, oligoclase and andesine, the plagioclase-bound Eu should be effected. The consistency in the Eu anomalies suggest that there must be the retention of plagioclase-bound Eu, probably locked in other phases in the ground mass, during the transformation of primary calcic-plagioclase to its altered products (see Whitford et al., 1988). It is interesting to note that none of these rocks display a Ce anomaly, as noted in various island arc suites such as Marianas (Hole et al., 1984), Solomon islands (Jakes & Gill, 1970) and central Japan (Masuda, 1968).

## DISCUSSION

### Tectonic affinity

Discussion of the chemical composition and magmatic affinity of metavolcanics from Dir area is complicated by the probability that some of the elements have been mobile during the secondary processes which the rocks have suffered and hence, the present chemical character of such rocks is function both of these events and primary magmatic processes.

Large ion lithophile elements (LILE) such as K, Rb, Na, Ba in the Dir metavolcanic sequence exhibit incoherent scatter on variation diagrams. However, the fact that the LILE are commonly remobilized during alteration and metamorphism renders them suspect in petrogenetic studies (Gelinas et al., 1982; Ludden et al., 1982; Vance & Condie, 1987). The high field strength (HFS) incompatible elements such

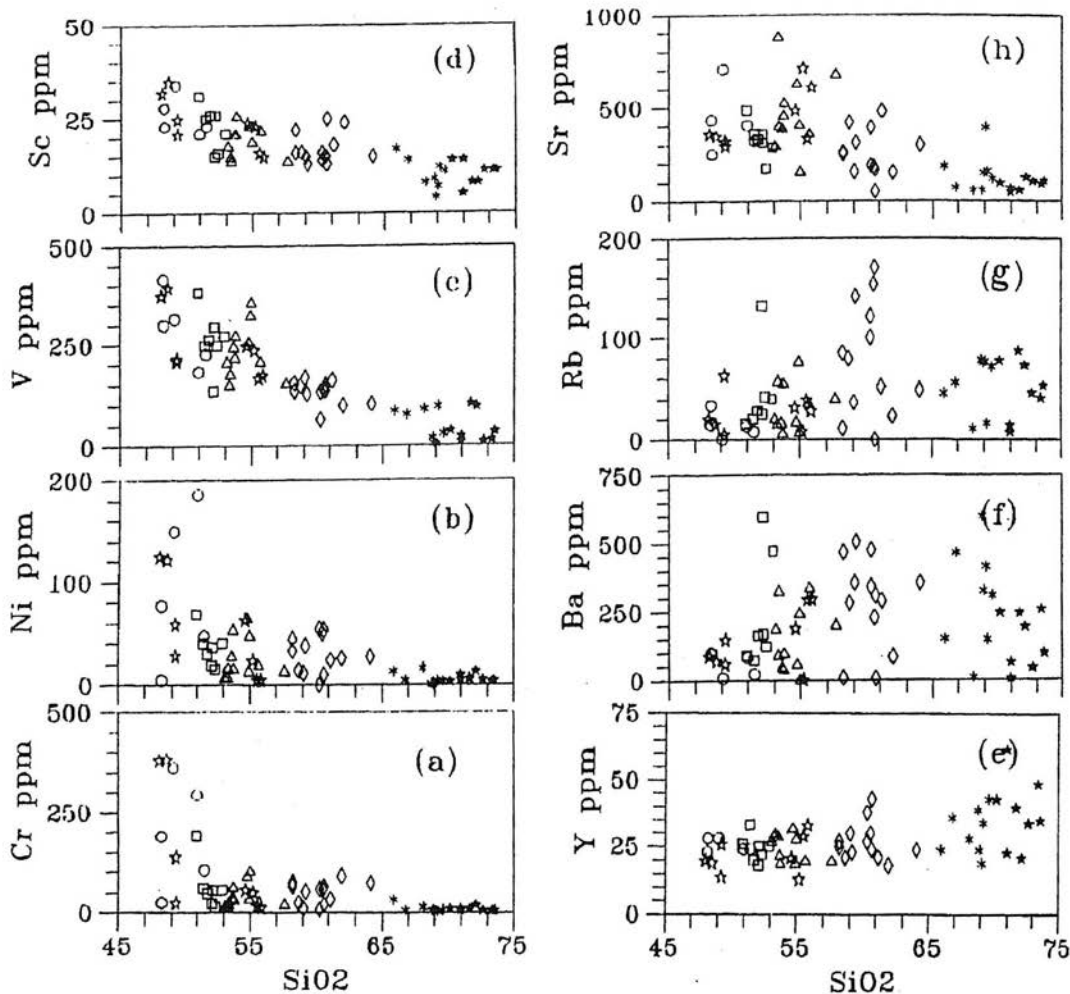


Fig. 4. Variation diagram of trace elements vs silica for the rocks of the Dir metavolcanic sequence. (Symbols as for Fig. 2).

as Ti, P, Zr, Nb, Y and the compatible elements (i.e. V, Ni, Cr, Sc & Co) preserve strong linear correlation and appear to be largely unaffected by secondary processes. The behavior of LILE and HFS elements in the Dir metavolcanics is consistent with the observation of previous workers on such kinds of low grade metamorphosed and altered rocks (Field & Elliott, 1974; Winchester & Floyd, 1976; Hanson, 1980). Both the incompatible and compatible HFS elements are, therefore, utilized in assess-

ment of petrogenetic discrimination techniques already established for defining the magma type and tectonic setting of the basic rocks either fresh or metamorphosed.

From the major and trace element variation diagrams we have already determined the calc-alkaline nature of the Dir metavolcanic sequence. The following discussion will further elaborate the petrogenesis of this sequence. On the Ti-Zr-Y, Ti-Zr-Sr and Ti-Zr tectonic characteristic diagrams (Fig. 7a-c) of Pearce and

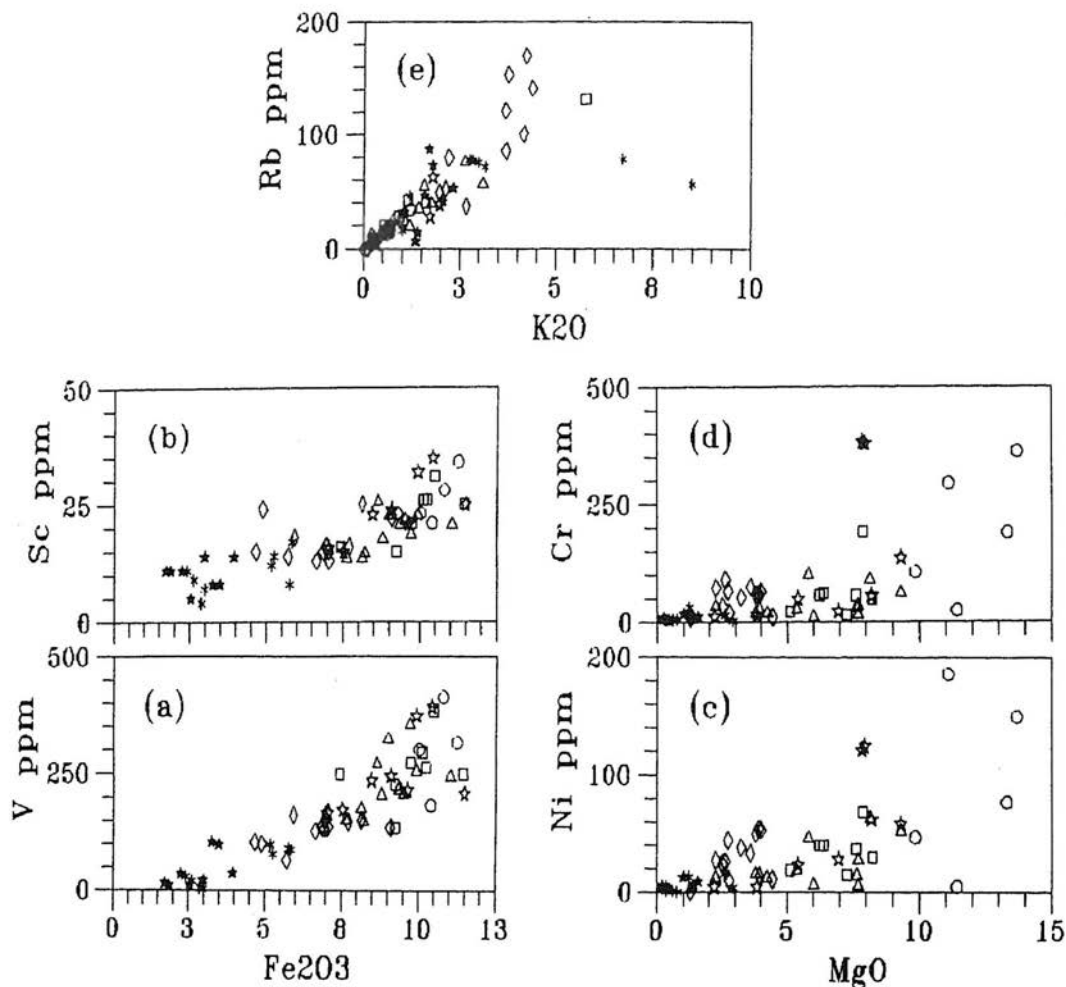


Fig. 5. Variation diagram of trace elements vs major elements for the rocks of the Dir metavolcanic sequence. (Symbols as for Fig. 2).

Cann (1973), most of the basalts to andesites concentrate within the field of calc-alkaline basalts. The use of tectonic environment discrimination diagrams involving Ti, Zr, Y, Cr and Sr suggest that the Dir metavolcanic sequence formed in an island arc type of setting.

Multi-elements diagrams are mostly used to illustrate the effects of source region composition on element abundances and their ratios. The average element abundances of individual members of the Dir metavolcanic sequence are

normalized to hypothetical primordial mantle composition of Wood et al. (1979) and plotted in order of increasing incompatibility for normal mantle mineral assemblages, from right to left in Figure 8a. It is apparent that the LILE (left hand side) increase relative to more compatible elements (on right hand side). The basalts (including pyroclastic breccia) and basaltic-andesites have small to negligible positive anomaly for Sr, while dacites and rhyolites have significant negative anomaly for Sr suggesting plagioclase accumulation to the mafic

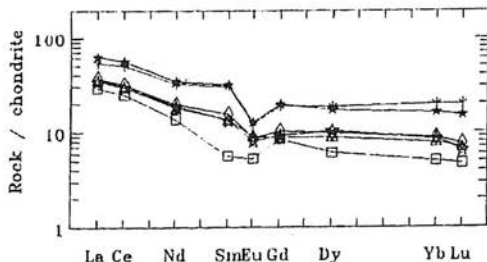


Fig. 6. Chondrite-normalized rare-earth element distribution for the selected samples from the rocks of the Dir metavolcanic sequence. (Symbols as for Fig. 2).

lavas and plagioclase fractionation from the felsic lavas. Ti has well developed negative anomaly in all the members of the sequence and is characteristic of magnetite/or titanomagnetite fractionation through out the sequence. Nb also has a negative anomaly in all the members of the sequence. These characteristics are typical of much of the complex, and impose some important constraints on the source and petrogenesis of the parent magma. Subduction related magmas have very low contents of Nb (Saunders et al., 1980), which results in the marked negative Nb anomaly on mantle-normalized diagrams. This is, therefore, a characteristic feature of subduction-related magmas, either in island arc or continental margin. In contrast, MORB has either no Nb anomaly or have positive Nb anomaly, while ocean island basalts have marked positive Nb anomalies. Negative Nb anomalies have also been noticed in the basalts from other tectonic settings such as back arc basins (especially during early stages of back arc spreading) and in ophiolites that have an arc origin (e.g. Troodos complex). The negative Nb anomaly and the high LIL/HFS element ratio in all the members of the Dir metavolcanic sequence confirm its relation with the subduction-related environment.

A MORB-normalized plot (Fig. 8b), using the normalization factors of Pearce (1983),

has also been constructed for the Dir metavolcanic sequence. The order of element in this plot is based upon their relative mobility in aqueous fluids which should control enrichment processes in subduction-related environment. All the samples show the same general features, namely enriched large ion lithophile element (LILE) concentrations relative to the less mobile (right hand side) REE and negative anomalies for Nb and Ti in all the members, and negative Sr anomalies in dacite and rhyolite. The MORB-normalized data further show many features typical of calc-alkaline suite in general.

It is clear from the above discussion that the behavior of various trace elements and REE in the metavolcanic sequence corresponds to a subduction-related magmatism of calc-alkaline nature.

### Crystal fractionation

The observed chemical trends of major and trace elements suggest the early removal of olivine which caused the rapid drop of MgO down to 50-55 wt.% Si<sub>2</sub>O (Figs. 2-4). This is followed by clinopyroxene and plagioclase fractionation. Magnetite and/or titanomagnetite started crystallizing at an early stage and depleted the residual liquid in Fe and Ti. This indicates oxidizing conditions, characteristic of the calc-alkaline suites (Osborn, 1962; Miyashiro, 1974). The negative correlations between compatible elements (Cr, Ni, V, and Sc and SiO<sub>2</sub>) in Figure 4 also reflect the removal of dominant clinopyroxene and magnetite/or titanomagnetite. The progressive depletion of V through out the metavolcanic sequence implies the removal of magnetite or titanomagnetite through crystal fractionation as it is also shown by Ti<sub>2</sub>O<sub>3</sub> and Fe<sub>2</sub>O<sub>3</sub> depletion in these rocks (basalts to rhyolite).

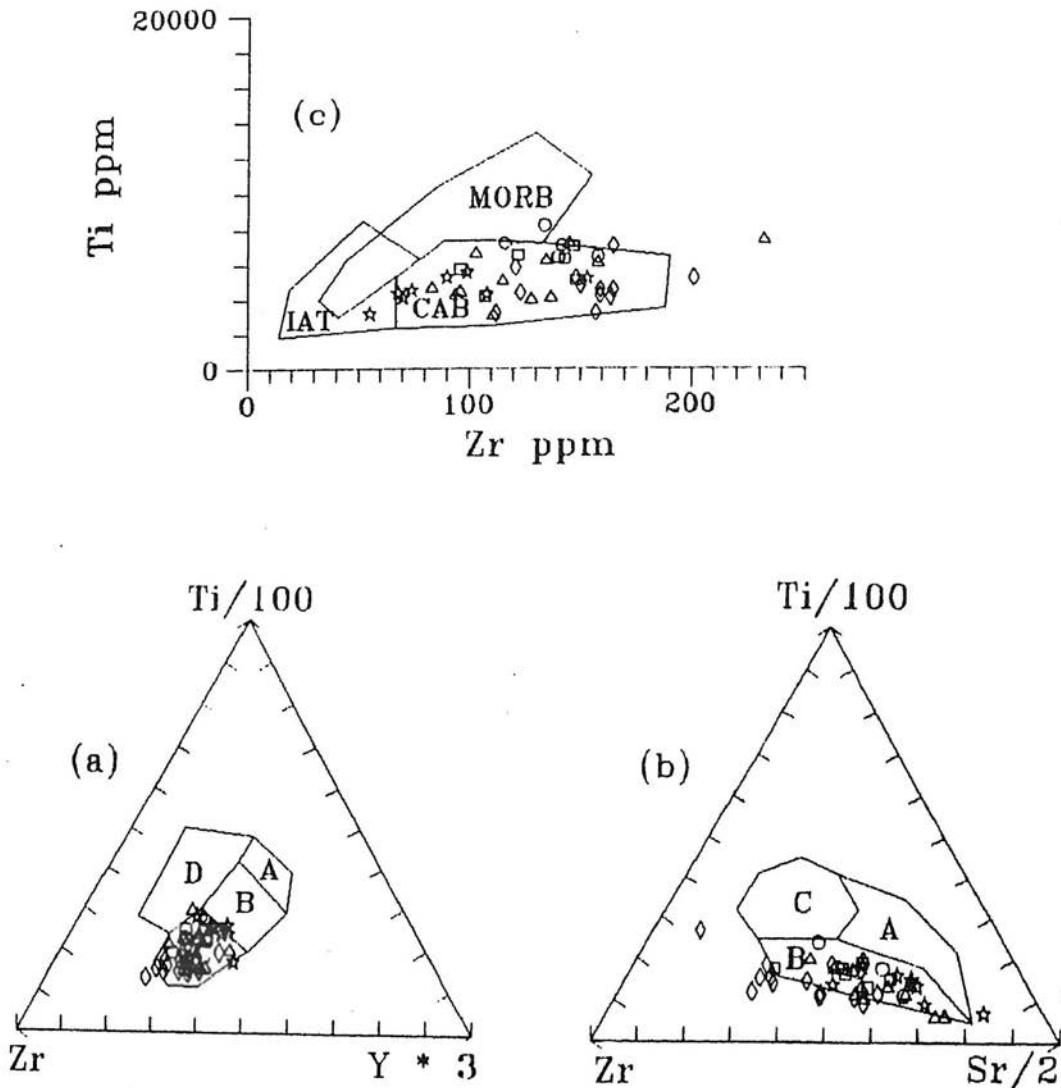


Fig. 7. Ternary diagrams of Pearce and Cann (1973) for basalts, basaltic-andesites and andesites of the Dir metavolcanic sequence. (Symbols as for Fig. 2).

a). Ti/100-Zr-Y<sup>3</sup> diagram

A+B = low-k tholietes

B = ocean floor basalt

b). Ti-Zr-Sr diagram

A = island arc basalt

C = ocean floor basalt

c). Ti-Zr diagram

B+C = calc-alkaline basalt

D = within plate basalt

B = calc-alkaline basalt

The linear array on element-element variation diagrams of both major and trace elements which define the liquid line-of-descent

for the Dir metavolcanic sequence and its calc-alkaline REE pattern suggest that the fractional crystallization have played an important role in

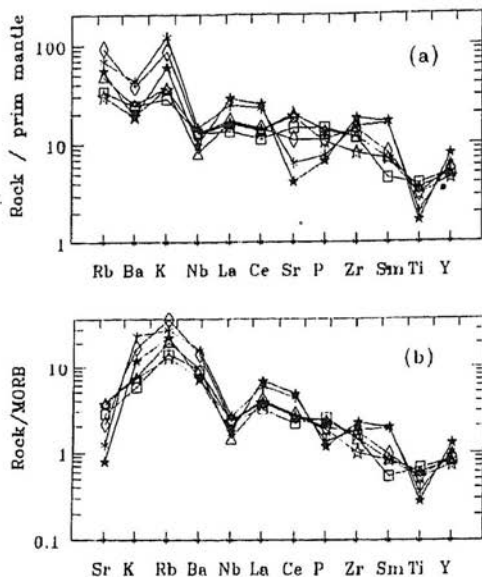


Fig. 8. Average trace elements distribution, normalized to (a) Premordial Mantle values of Wood et al., (1979) and (b) MORB values as cited in Pearce, (1983) for the Dir metovolcanic sequence. (Symbols as for Fig. 2).

the development of the various members of the sequence.

### Petrogenesis

The composition and origin of primary island arc magmas is a main concern of the present day petrologists. As we gain more petrological, geochemical and geophysical information about the world's active volcanic arcs, new ideas have developed on many fundamental aspects of island arc petrogenesis. On one hand, the great volume of high alumina basaltic (HAB) lavas are considered to be the primary parental arc magmas generated by the partial melting of subducted oceanic crust or quartz eclogite (Marsh, 1979; Brophy & Marsh, 1986; Borphy, 1986; Myers et al., 1986). On the other hand, the sporadic occurrence of basalts with more primitive (MgO rich) characteristics provide evidence for the existence of mantle derived

olivine tholeiite parental basalt ( $Mg\# > 65$ ) from a source similar to that of ocean ridge tholeiites. In the latter case the high alumina basalts has been considered to be a derivative of the primary magma through extensive fractionation, dominated by olivine and clinopyroxene. These primary, high magnesia basalts are thought to be generated by partial melting of peridotite in the mantle wedge above the descending slab of subducted oceanic crust (see Gill, 1981; Ramsay et al., 1984; Crawford et al., 1987; Gust & Perfit, 1987).

Geochemical data of the Dir metovolcanic sequence is used here to test whether or not the high-alumina basalt could be the parent magma from which the other members of the sequence evolved.

Average high-magnesia basalts, low-magnesia basalts, pyroclastic breccia and basaltic andesites have been plotted in a plot of  $Al_2O_3$  vs  $Mg\#$  (Fig. 9; after Gust & Perfit 1987) to further evaluate the parent/daughter relationship of these rock types. The average high-magnesia basalt from the Dir area lies very close to the

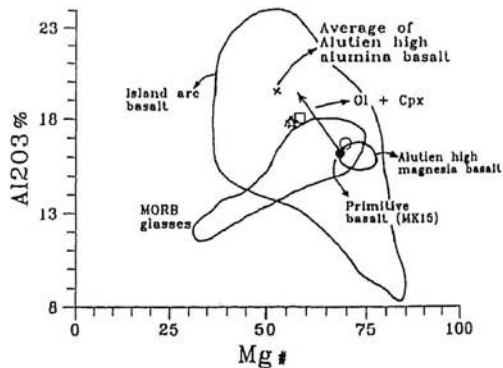


Fig. 9. Average of high-magnesia basalt, low-magnesia basalt, pyroclastic breccia and basaltic-andesite are plotted in the  $Al_2O_3$  (wt.%) vs  $Mg\#$  diagram. Various fields and the vector representing the fractional crystallization of 10% olivine + 6% clinopyroxene from parental basalt are after Gust & Perfit, (1987). (Symbols as for Fig. 2).

field marked for the Aleutian high-magnesia basalt, and also to relatively primitive basalt (MK15 with MgO > 9 wt.%), which Gust and Perfit (1987) used as starting material in their experiment to generate high alumina basalt at moderate pressure under essentially anhydrous condition. The average low-magnesia basalts, the pyroclastic breccia and basaltic-andesites plot within the field marked for island arc basalt and in close proximity with that of the average high alumina basalt (HAB) of the Aleutian island arc (Fig. 9). These rocks also lie either on or close to the calculated line for 10% olivine + 6% clinopyroxene fractionation from the parental basalt (MK15) of Gust and Perfit (1987). This suggests the possible derivation of low-magnesia basalts, pyroclastic breccia and basaltic andesites of Dir area from the high-magnesia basalt by simple fractionation of olivine and clinopyroxene (+spinel) from the later type (see Crawford et al., 1987; Gust & Perfit, 1987).

The primary nature of these high-magnesia basalts is still uncertain. Past studies of high-pressure phase equilibria, however, suggest that a primary MORB picrite (14 wt.% MgO) can be produced by partial melting at a depth between 50 and 80 km (Ethon & Scarf, 1984). The generation of MORB (10 wt.% MgO) from spinel lherzolite at depth around 35 km has been indicated by Fujii and Scarfe (1985). The high-Mg basaltic composition of primary magmas and their generation within the modified mantle diapirs at a depth between 35 to 70 Km has been suggested by Tatsumi et al. (1983).

It is suggested that high-magnesia basalts of the Dir area are primitive in nature and may represent a primary magnesian liquid produced by the partial melting of peridotitic mantle wedge at the base of the Kohistan island arc and above the subducted oceanic crust of the

Indo-Pakistan plate. This led to the formation of low-magnesia basalt (both basaltic flows and pyroclastic breccia) which further evolved to other members especially the basaltic-andesite.

**Acknowledgement:** We are very thankful to the Sarhad Development Authority (SDA), for providing assistance to the principal author during field work. Thanks are also due to Mr. Nawaz Khan and Mr. Noroz Khan, from SDA, for their help and nice hospitality during field work. Analytical facilities were provided by the Geochemistry Laboratory, Eastern Washington University and Department of Geological Sciences, University of South Carolina. Financial support for this research was provided by the National Science Foundation grant INT-8813655 (to J.W.S) and the United State Agency for International Development (to M.T.S), which is gratefully acknowledged.

## REFERENCES

- Bard, J. P., 1983. Metamorphism of an obducted island arc; example of the Kohistan sequence (Pakistan) in Himalayan collided range. *Earth. Planet. Sci. Lett.*, 65, 113-144.
- Borphy, J. G., 1986. The Cold Bay volcanic center, Aleutian volcanic arc. *Contrib. Mineral. Petrol.*, 93, 368-380.
- Borphy, J. G. & Marsh, B. D., 1986. On the origin of high-alumina arc basalt and the mechanics of melt extraction. *Jour. Petrol.*, 27, 763-789.
- Cann, J. R., 1970. Rb, Sr, Y, Zr and Nb in some ocean floor basaltic rocks. *Earth. Planet. Sci. Lett.*, 10, 7-11.
- Cornad, W.K. & Kay, R.W., 1984. Ultramafic and mafic inclusions from Adak island: crystallization history and implications of primary magmas and crustal evolution in the Aleutian arc. *Jour. Petrol.*, 25, 245-266.
- Coward, M. P., Windley, B. F., Broughton, R. D., Luff, I. W., Petterson, M. G., Pudsey, C. J., Rex, D. C. & Khan, M. A., 1986. Collision tectonic in the NW Himalayas. In: *Collision Tectonics* (M. P. Coward & A. C. Ries, eds.). *Geol. Soc. London. Spec. Pub.*, 19, 203-209.

- Crawford, A. J., Greene, H. G. & Exon, N., 1987. Geology petrology and geochemistry of submarine volcanoes around Epi Island (Vanatu). In: Geology and offshore resources of Pacific island arcs. The New Hebrides region: Circum-pacific (H. G. Greene & F. Wong, eds.). Earth and Science Series.
- Crock, J. G. & Lichte F. E., 1982. Determination of rare earth elements in geological materials by inductively coupled argon plasma/atomic emission spectrometry. *Anal. Chem.*, 54, 1329-1332.
- Feild, D. & Elliott, R.B., 1974. The chemistry of gabbro/ampibolite transitions in South Norway. *Contrib. Mineral. Petrol.*, 38, 71-79.
- Fletcher, C. J. N., 1985. Copper mineralization in the Kohistan Complex, near Dir and Drosh, North-west Frontier Province. *Brit. Geol. Surv.*, 1-65.
- Fujii, T. & Scarf, C. M., 1985. Composition of liquids coexisting with spinel lherzolite at 10 Kbar and the genesis of MORBS. *Contrib. Mineral. Petrol.*, 90, 18-28.
- Gelinas, L., Mellinger, M. & Trudel, P., 1982. Archaean mafic metavolcanics from the Rouyn-Noranda district, Abitibi greenstone belt, Quebec, 1. Mobility of the major elements. *Canad. Jour. Earth. Sci.*, 19, 2258-2275.
- Gill, J. B., 1981. Orogenic Andesites and plate tectonics. Springer Berlin Heidelberg, New York. 390p.
- Gust, D. A. & Perfit, M. R., 1987. Phase relation of high-Mg basalt from the Aleutian island arc: implication for primary island arc basalt. *Contrib. Mineral. Petrol.*, 97, 7-18.
- Hamidullah, S., Islam, F. & Farooq, M., 1992. Petrology and geochemistry of the western part of Kalam-Dir igneous complex, Kohistan arc, northern Pakistan. In: Geology and geodynamic evolution of the Himalayan collision zone (K. Sharma, ed.). *Physics and Chemistry of the Earth*, 17, 31-46.
- Hanson, G. N., 1980. Rare earth elements in petrogenetic studies of igneous systems: *Annual Rev. Earth Planet. Sci. Lett.*, 8, 371-406.
- Hole, M. J., Saundes, A. J., Marriner, G. F. & Tarney, J., 1984 Subduction of pelagic sediments; implication for the origin of Ce-anomalous basalts from Mariana Islands. *Jour. Geol. Soc. Lond.* 141, 453-472.
- Irvine, T. N. & Barager, W. R. A., 1971. A guide to the chemical classification of the common volcanic rocks. *Canad. Jour. Sci.*, 8, 523-548.
- Jakes, P. & Gill, J. B., 1970. Rare earth element and the island arc tholeiite series. *Earth Planet. Sci. Lett.*, 9, 17-28.
- Kakar, S. K., Mian, S. B. & Khan, J., 1971. The geology of Jandul valley, western Dir. *Geol. Bull. Univ. Peshawar*, 6, 54-73.
- Khan, M. A., 1979. Geology of the Baraul Valley, Dir. *Geol. Bull. Univ. Peshawar*, 11, 153-162.
- Majid, M. & Paracha, F. A., 1980. Calc-alkaline magmatism at the destructive plate margin in Kohistan Pakistan. *Geol. Bull. Univ. Peshawar*, 13, 109-120.
- Majid, M., Shah, M. T., Latif, A., Aurangzeb. & Kamal, M., 1981. Major elements abundance in the Kalam lavas. *Geol. Bull. Univ. Peshawar*, 14, 45-62.
- Marsh, B. D., 1979. Island arc development: some observations, experiments and speculations. *Jour. Geol.*, 87, 687-713.
- Marsh, B. D., 1979. Island arc development: some observations, experiments, and speculation. *Jour. Geol.*, 87, 687-714.
- Masuada, A., 1968. Geochemistry of Lanthanides in basalts of central Japan. *Earth Planet. Sci. Lett.*, 4, 284-292.
- Miyashiro, A., 1974. Volcanic rock series in island arc and active continental margins. *Amer. Jour. Sci.*, 274, 321-355.
- Myers, J. D., 1988. Possible petrogenetic relations between low and high-MgO Aleutian basalts. *Geol. Soc. Amer. Bull.* 100, 1040-1053.
- Myers, J. D., Frost, C. & Angevine C. L., 1986. A test of a quartz eclogite source for parent Aleutian magma: a mass balance approach. *Jour. Geol.*, 94, 811-828.
- Nakamura, K., 1974. Determination of REE, Ba, Fe, Mg, Na and K in carbonaceous and ordinary chondrites. *Geoch. et. Cosmoch. Acta.*, 38, 757-775.

- Osborn, E. F., 1962. Reaction series for subalkaline igneous rocks based on different oxygen pressure conditions. *Amer. Mineral.*, 47, 211-216.
- Pearce, J. A., (1975) Basalt geochemistry used to investigate past tectonic environments on Cyprus. *Tectonophysics*, 25, 41-67.
- Pearce, J. A., 1983. Role of the sub-continental lithosphere in magma genesis at active continental margins. In: *Continental Basalt and Mantle Xenoliths* (C. J. Hawkesworth & M.J. Norry, eds.). Shiva, Nantwich, 230-249.
- Pearce, J. A. & Cann, J. R., 1973. Tectonic setting of basic volcanic rocks determined using trace element analyses. *Earth Planet. Sci. Lett.*, 19, 290-300.
- Perfit, M. R., Gust, D. A., Bence, A. E., Arculus, R. J. & Taylor, S. R., 1980. Chemical characteristics of island-arc basalts: implications for mantle sources: *Chem. Geol.*, 30, 227-256.
- Pudsey, C. J., 1986. The northern suture, Pakistan; margin of the Cretaceous island arc: *Geol. Mag.*, 123, 405-423.
- Rabi, F., Khattah, N., 1983. Petrography and geochemistry of diorites and volcanics from northern Dir. Unpubl. M.Sc. thesis, Peshawar University.
- Ramsey, W. R. N., Crawford, A. J. & Foden, J. D., 1984. Field setting, mineralogy, chemistry and genesis of arc picrite. New Georgia, Solomon Islan. *Contrib. Mineral. Petrol.*, 88, 386-402.
- Saunders, A. D., Tarney, J. & Weaver, S. D., 1980. Transverse variation across the Antarctic Peninsula: implications for the genesis of calc-alkaline magmas. *Earth. Planet. Sci. Lett.*, 46, 344-360.
- Shah, M. T., 1991. Geochemistry, Mineralogy and petrology of the sulfide mineralization and associated rocks in the area around Besham and Dir, northern Pakistan. Unpubl. Ph.D. thesis, Univ. of South Carolina, Columbia, U.S.A.
- Shah, M. T. & Shervais, J. W., 1991. Petro-chemical evolution of the Dir metavolcanic sequence, Kohistan arc terrane, northern Pakistan. *Geol. Soc. Amer. Abst.*, 23, A391p.
- Shah, M. T., Shervais, J. W. & Ikramuddin, M., 1990. Geochemistry of metavolcanics and associated Cu-mineralization in the Dir area of Kohistan island arc, N. Pakistan. *Geol. Soc. Amer. Abst.*, 22, A363p.
- Sullivan, M., Windley, A. D., Saunders, A. D., Haynes, J. R. & Rex, D. C., 1992. A palaeogeographic reconstruction of the Dir group: evidence for magmatic arc migration within Kohistan, N. Pakistan. In: *Himalayan Tectonics* (P.J. Treloar, & M.P. Searl, eds.). *Geol. Soc. Spec. Publ.* 74, 139-160.
- Tahirkheli, R. A., Mattauer, M., Proust, F., & Tapponnier, P., 1979. The India-Eurasia suture zone in northern Pakistan; synthesis and interpretation of recent data at plate scale. In: *Geodynamic of Pakistan*. (A. Farah & K. DeJong eds.). *Geol. Surv. Pakistan*, 125-130.
- Tatsumi, Y., Sakuyama, M., Fukuyama, H. & Kushiro, I., 1983. Generation of arc basalt magmas and thermal structure of the mantle wedge in subduction zone. *Jour. Geophys. Res.*, 88, 5815-5825.
- Treloar, P. J., Rex, D. C., Guise, P. G., Coward, M. P., Searle, M. P., Windley, B. F., Petterson, M. G., Jan, M. Q. & Luff, I. W., 1989. K-Ar and Ar-Ar geochronology of the Himalayan collision in NW Pakistan: constraints on the timing of suturing, deformation, metamorphism and uplift. *Tectonics*, 8, 881-909.
- Vance, R. K. & Condie K. C., 1987. Geochemistry of foot-wall alteration associated with the early proterozoic united verde massive sulfide deposits, Jerome Arizona. *Econ. Geol.*, 82, 571-586.
- Whitford, D. J., Korsch, M. J., Porritt, P. M. & Craven, S. J., 1988. Rare earth element mobility around the volcanogenic polymetallic massive sulfide deposit at Que river, Tasmania, Australia. *Chem. Geol.*, 68, 105-119.
- Winchester, J. A. & Floyd, P. A., 1976. Geochemical magma type discrimination: application to altered and metamorphosed basic igneous rocks. *Earth Planet. Sci. Lett.*, 28, 459-469.
- Wood, D. A., Tarney, J., Varet, J., Saunders, A. D., Bougault, H., Joron, J. L., Treuil, M. & Cann, J. R., 1979. Geochemistry of basalt drilled in the north Atlantic by IPOD leg 49: implication for mantle heterogeneity. *Earth Planet. Sci. Lett.*, 42, 77-97.